The Hubble constant from near-infrared observations of type Ia supernovae

Lluís Galbany, ICE-CSIC (Barcelona)

CosmoVerse, Napoli, 2025 May 23rd

Institute of Space Sciences

IEEC

CSIC
Consejo Superior de Investigaciones Científicas

Ministerio de Ciencia e Innovación

Unión Europea
Fondo Social Europeo
El FSE invierte en tu futuro

Agencia Estatal de Investigación

Context: Type Ia supernova

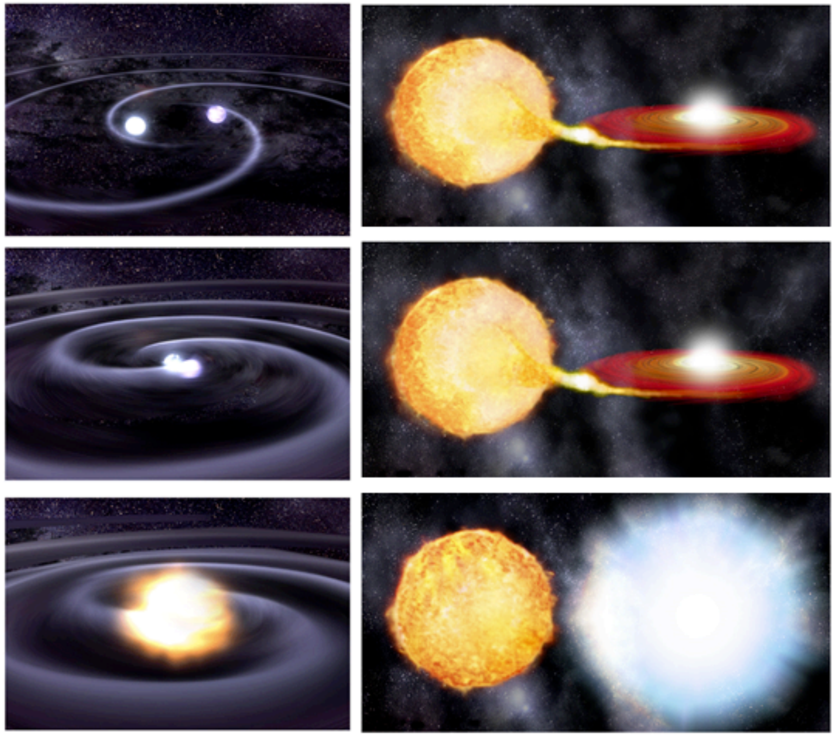

What is exploding?

CO white dwarf (WD) in a binary system
single/double/core degenerate

How is it exploding?

Merging/compression/He layer burn/collision
Detonation/deflagration/double-detonation
Chandrasekhar/sub-Chandrasekhar mass

Most probably a mixture of scenarios and explosion mechanisms

SNIa are the most precise extragalactic distance indicators (uncert. ~5%)

$$\mu(z) = m(z) - M$$

No evolution: $SNIa_{low} \sim SNIa_{high}$

Same populations: $p(SNIa_{low}) \sim p(SNIa_{high})$

OPTICAL

Context: Type Ia supernova parametrization

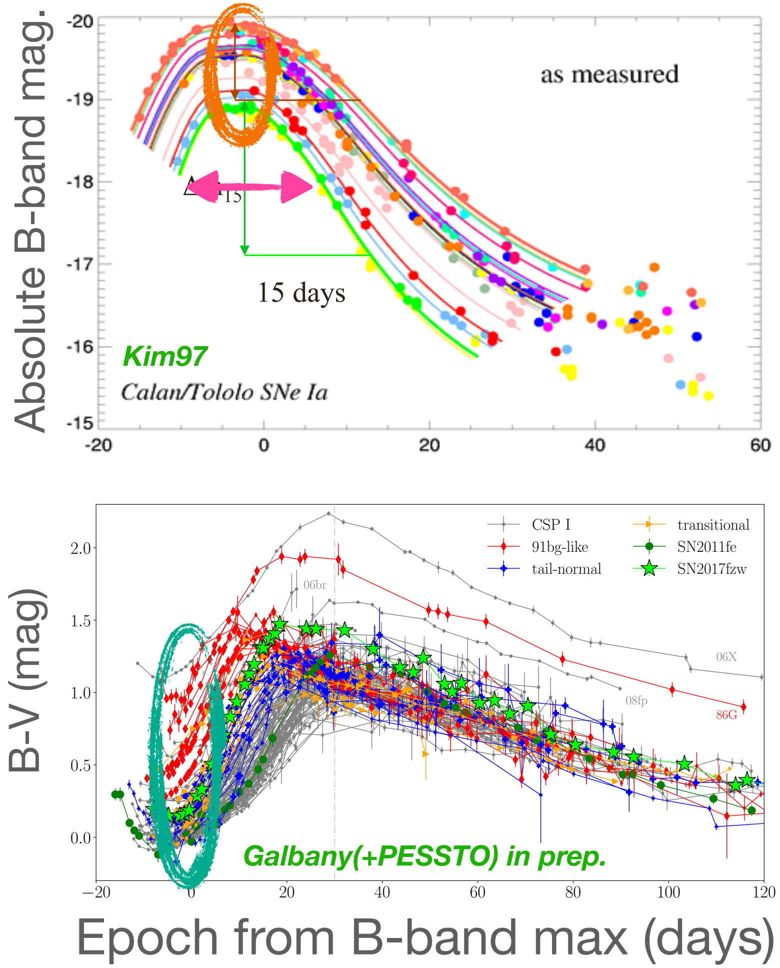

Light-curve parametrization:

- m_B^{max}, peak magnitude
- $\Delta m_{15}(B)$, $x1$, s_{BV}, width
- $E(B-V)_{max}$, c, color

Progenitor scenario
explosion mechanism
progenitor mass
extinction

$+\alpha\ x1 \quad +\beta\ c$

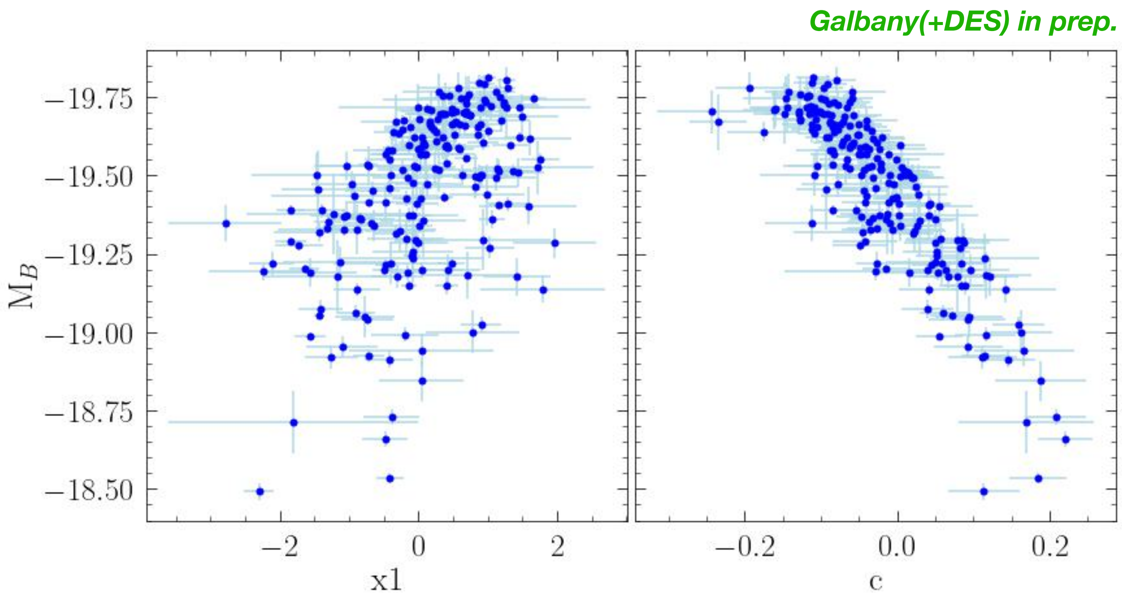

OPTICAL

Context: SNIa cosmology

Hubble diagram and *residual*

$$\mu(z)_{\text{observed}} = m(z) - M + \alpha x1 - \beta c$$

$$\mu(z)_{\text{model}} = 5\log_{10}(d_L/10\text{pc})$$

$$d_L(z) = (1+z)\frac{c}{H_0}\int_0^z \frac{dz}{\sqrt{\Omega_M(1+z)^3 + \Omega_\Lambda(a+z)^{3(1+w)}}}$$

$$HR = \mu(z)_{\text{obsereved}} - \mu(z)_{\text{model}}$$

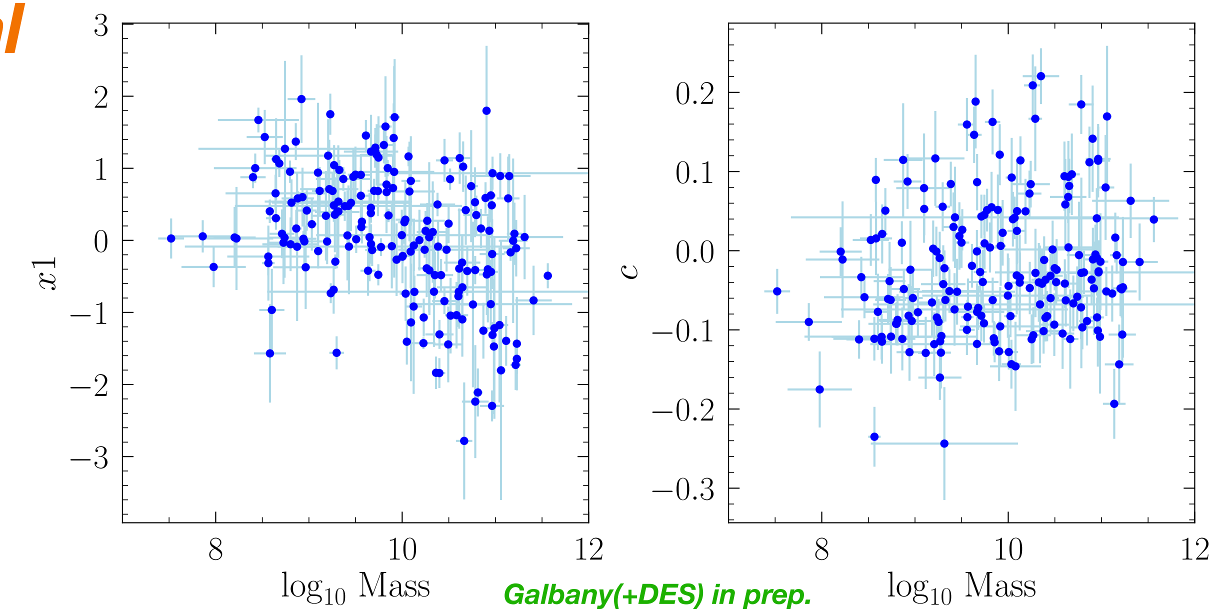

Galbany(+DES) in prep.

Recent (>2010) cosmological analysis found a dependence between the *HR* and $\boxed{\text{properties of the SN host galaxy}}$ $+\gamma M_*$

OPTICAL

Context: SNIa environments

Dependences of the SN parameters on host galaxy properties

As they evolve with redshift, such dependences would impact the cosmological parameters

Hamuy et al. (1996)	Bright events occur preferentially in **young** stellar environments.
Hamuy et al. (2000)	Luminous SNe are produced in **metal-poor** neighborhoods
Gallagher et al. (2005)	**high-metallicity** galaxies host SNe Ia with negative HR *(after LC-corr)*
Sullivan et al. (2006)	Brighter events are found in systems with ongoing **star-formation**
Gallagher et al. (2008)	**Progenitor age** primarily determines the peak luminosity
Hicken et al. (2009)	SN Ia in **spiral** hosts are intrinsically fainter *(after LC-corr)*
Howell et al. (2009)	**more massive** progenitors give rise to less luminous explosions
Neill et al. (2009)	**Older** hosts produce less-extincted SNe Ia
Cooper et al. (2009)	SNIa are more luminous or more numerous in **metal-poor** galaxies
Brandt et al. (2010)	Luminous SNe associated with recent **star-formation** and **young** prog.
Sullivan et al. (2010)	SNIa are brighter in **massive** hosts (metal-rich) and with low **SFR** *(after LC-corr)*
Kelly et al. (2010)	SN Ia in physically **larger**, more **massive** hosts are ~10% brighter
Lampeitl et al. (2010)	introduce the stellar **mass** of the host in the parametrization
D'Andrea et al. (2011)	SNe are 0.1 mag brighter in **high-metallicity** hosts after corr.
Gupta et al. (2011)	**older** galaxies host SNe Ia that are brighter
Konishi et al. (2011)	SNe Ia in host galaxies with a higher **star formation** rate show brighter events
Galbany et al. (2012)	SNe that explode **further** are less extinguished, and have **lower metallicity**
Childress et al. (2013)	correlation between SN Ia intrinsic color and host **metallicity**
Johansson et al. (2013)	more luminous SNe Ia appear in **younger** stellar progenitor systems
Rigault et al. (2013)	SNe Ia with **local Hα emission** are redder and drives the HR-**mass** relation
Pan et al. (2014)	fainter, faster declining SNe Ia are hosted by **older**/**massive**/**metal-rich** galaxies
…	

OPTICAL

Context: SNIa Hubble diagram

EXTRAGALACTIC ASTROPHYSICS → **COSMOLOGY**

SN progenitors
Environment
Dust

$$\mu = m - M \; +\alpha\, x1 \; +\beta\, c \; +\gamma\, M_*$$

Scolnic+18, Pantheon+

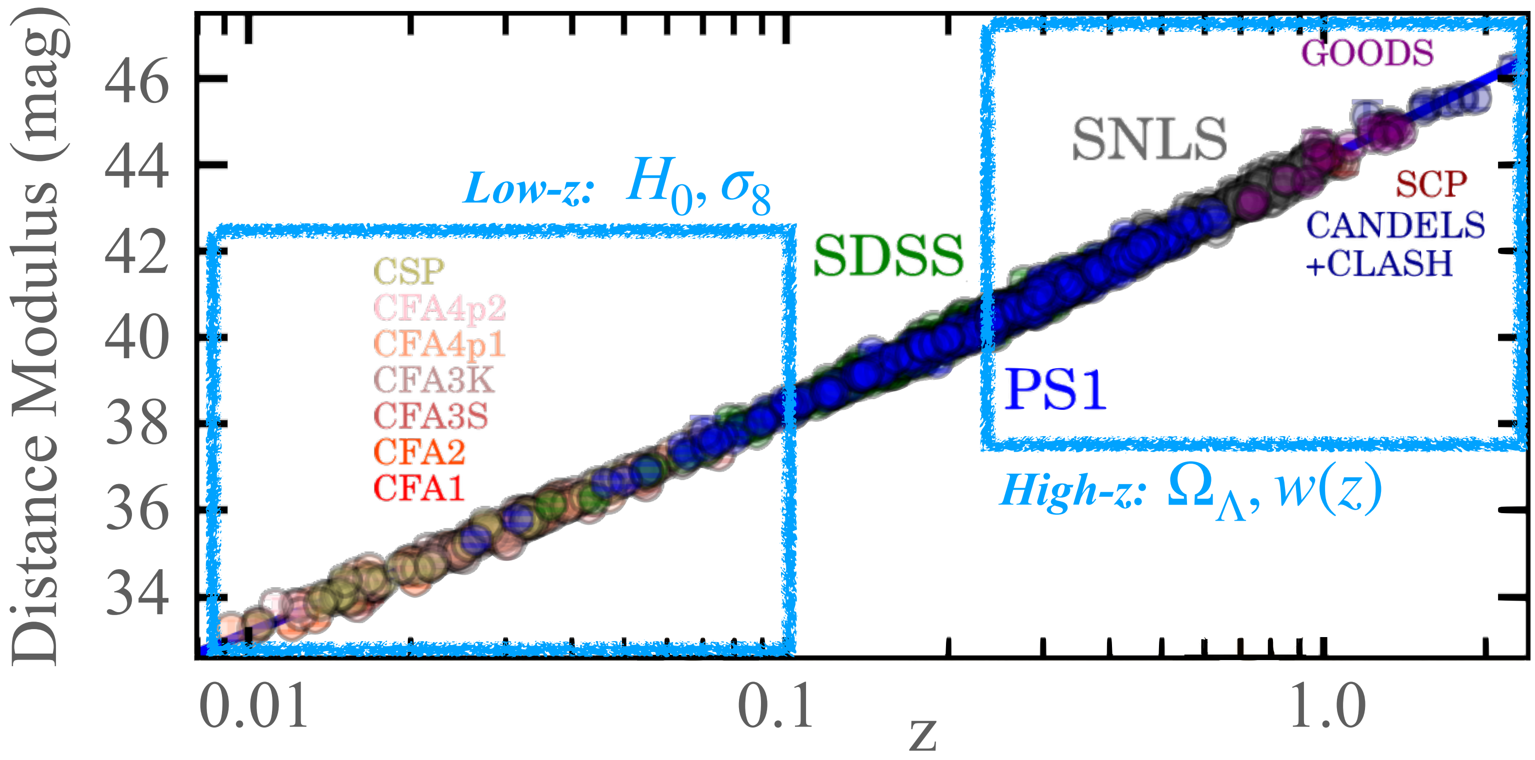

OPTICAL

Context: Systematics

$$\mu = m - M \quad +\alpha\ x1 \quad +\beta\ c \quad +\gamma\ M_*$$

α progenitor?

β dust/intrinsic

γ environment

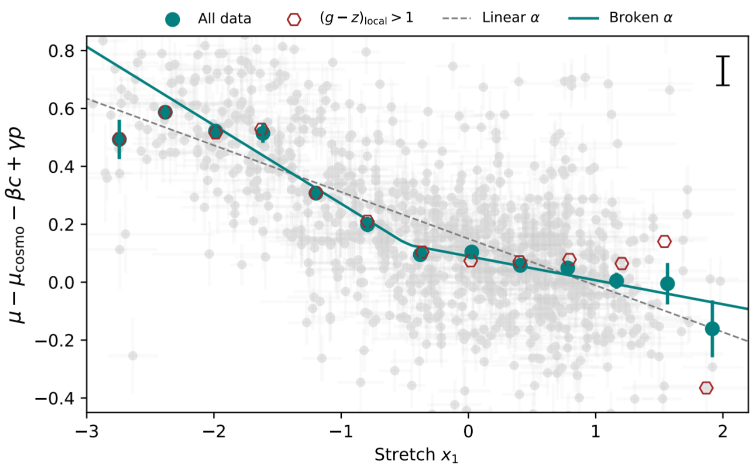

Ginolin+25

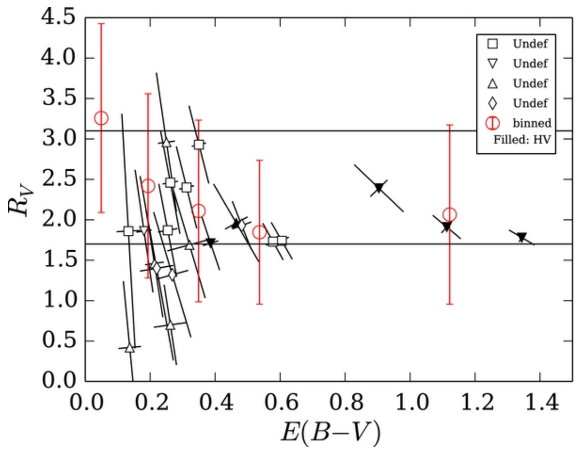

Burns+14

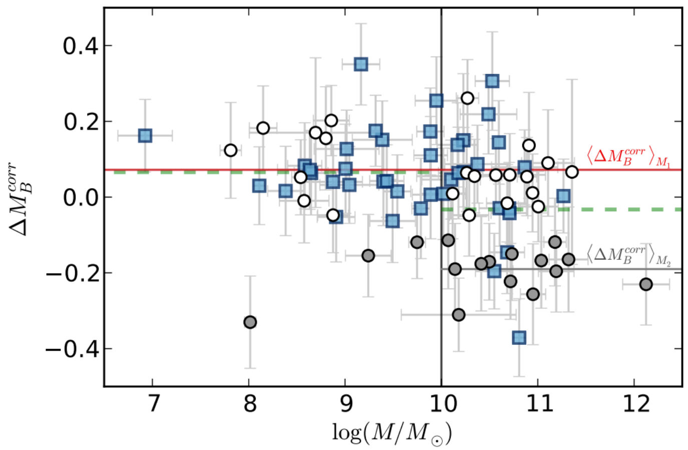

Rigault+13

SNIa in the NIR

Uniform light-curves (Elias+81, Elias&Frogel83)

Two Type I supernovae in NGC 1316 and one in NGC 4536 have been observed at *J*, *H*, and *K*. The data provide the best available Type I supernova light curves at these wavelengths. These light curves are characterized by a double maximum; the effect is strongest at *J*. This is probably due to the development of a transient absorption feature during the intervening minimum. The three sets of infrared light curves are very similar, and their dispersion in absolute magnitude is less than the uncertainty in relative distances of the supernovae. Infrared light curves of supernovae may therefore be useful as distance indicators within a few tens of Mpc.

Distinction between Ia / Ib (Elias+85)
double-peak (Fe recomb.)

TYPE I SUPERNOVAE IN THE INFRARED AND THEIR USE AS DISTANCE INDICATORS

J. H. Elias,[1] K. Matthews,[1] G. Neugebauer,[1] and S. E. Persson[2]

Received 1985 January 28; accepted 1985 March 22

New infrared data for 11 Type I supernovae are presented. These results, when combined with other published data for Type I supernovae, show that the light curves fall into two well-defined groups. The first, more common type—Type Ia—shows strong, variable, unexplained absorption at 1.2 μm and probably at 3.5 μm, while the second type—Type Ib—shows no such absorption and a slower decline after maximum. The light curves of the Type Ia supernovae appear to have a dispersion in color and absolute magnitude of ± 0.2 mag or less, making them potentially valuable for distance determination within the Local Supercluster.

Better distance indicators (Miekle+00)

The light curves of the six similar supernovae can be represented fairly consistently with a single light curve in each of the three bands. In all three IR bands the dispersion in absolute magnitude is about 0.15 mag, and this can be accounted for within the uncertainties of the individual light curves. No significant variation of absolute IR magnitude with *B*-band light curve decline rate, $\Delta m_{15}(B)$, is seen over the range $0.87 < \Delta m_{15}(B) < 1.31$. However, the data are insufficient to allow us to decide whether or not the decline rate relation is weaker in the IR than in the optical region. IR light curves of type Ia supernovae should eventually provide cosmological distance estimates that are of equal, or even superior, quality to those obtained in optical studies.

The promise of the NIR

Burns+18

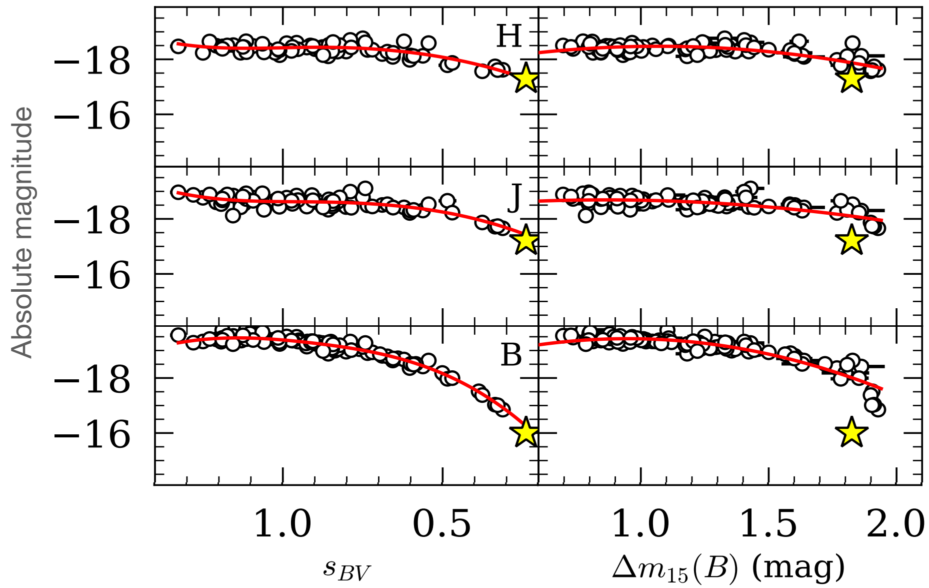

LC corrections in the NIR considerably smaller than in the optical

Extinction is much reduced in the NIR: A_H/A_V ~ 0.19 (Cardelli+89)

Uniform LCs

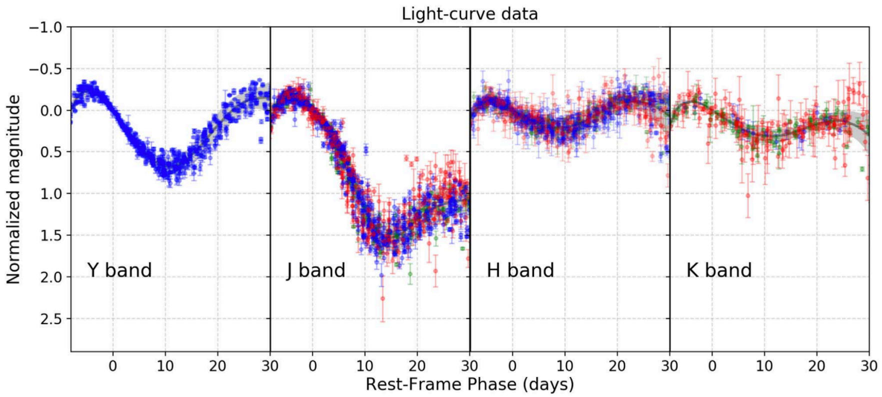

Avelino+19

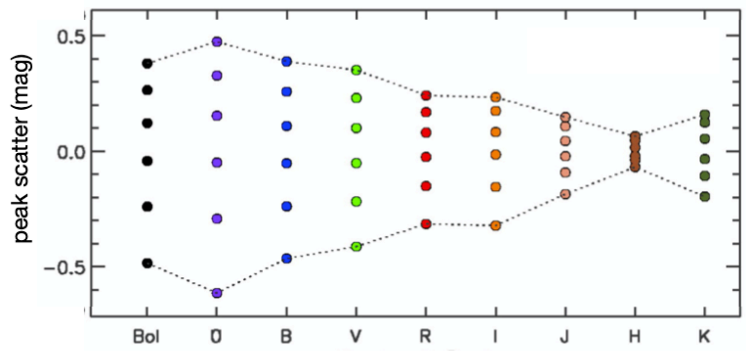

Kasen06

H_0 with SNe Ia in the NIR

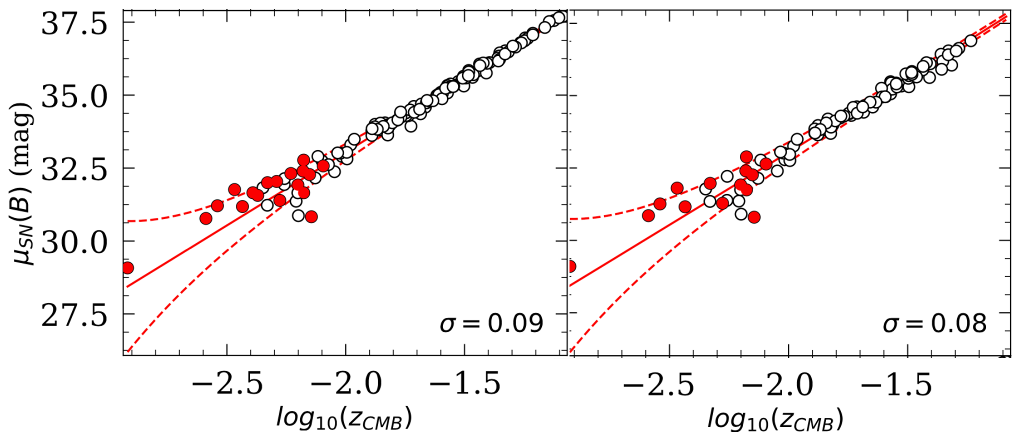

Burns+18 (*Uddin+24*), template fitting

15 (*20*) calibrators in the NIR

~100 (~*230*) Hubble flow SNIa

Dhawan+18, J-band interpolation

9 calibrators

27 Hubble flow SNIa

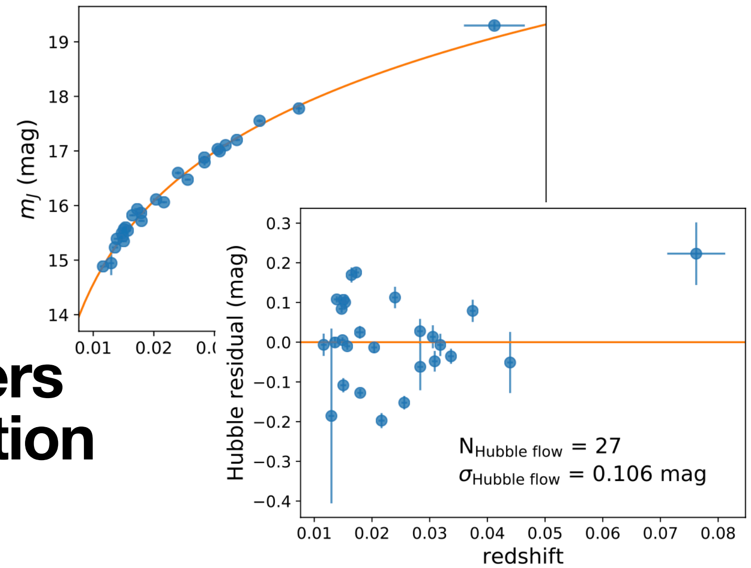

Uncertainties with 36 SNe Ia comparable to 200 SNe Ia in the optical

Systematic effects reduced: fewer free parameters (LC corrections) & decreased influence of extinction

LG, de Jaeger, Riess, et al. 2023A&A...679A..95G

H0 with SNe Ia in the NIR - an update

Increase sample: from SHOES R16 (19 cal.) to R22 (42 cal. in 38 gal.)
literature search of 57 SNe Ia in the Hubble flow

Include H-band

S-corrected photometry to the common CSP system

No template fitting, GP or simple spline (best chi2)

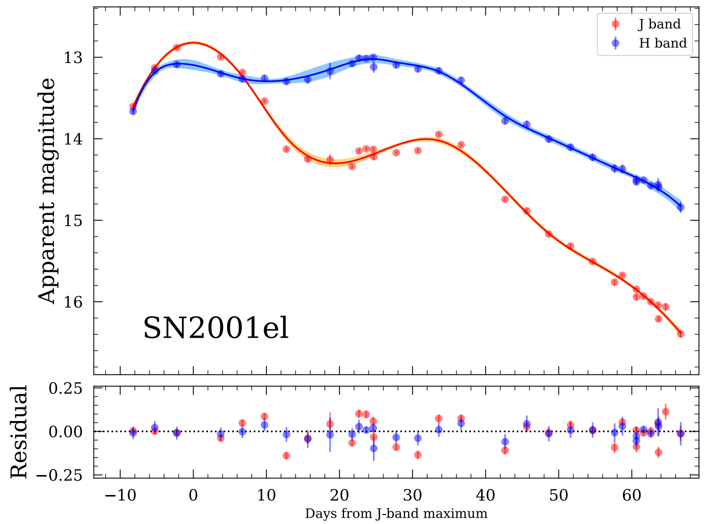

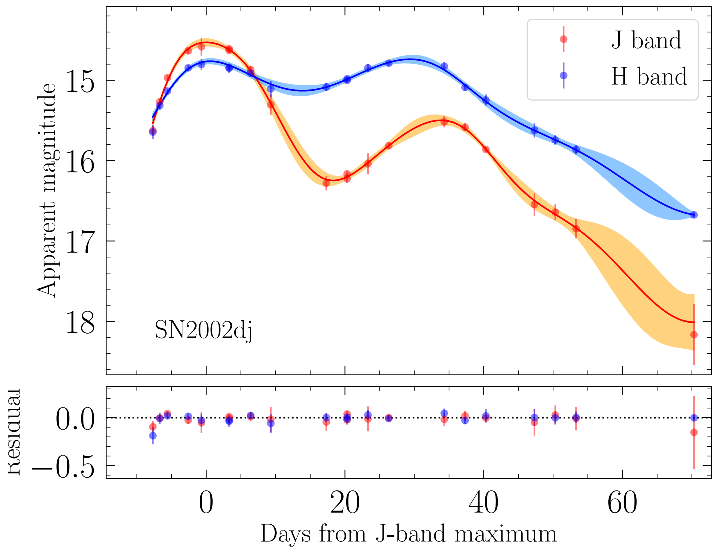

Calibrators

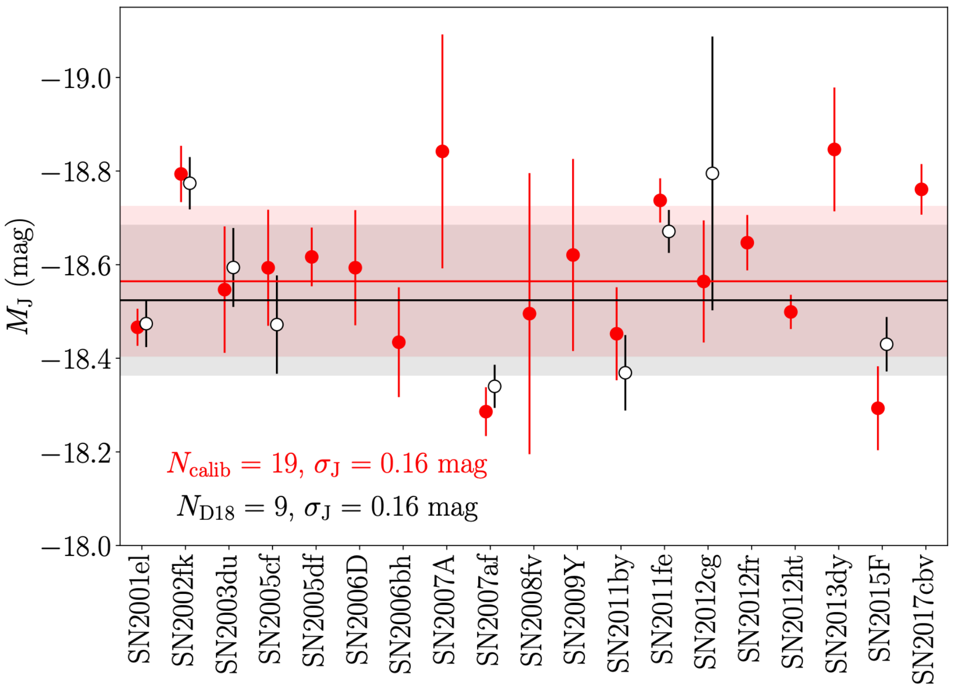

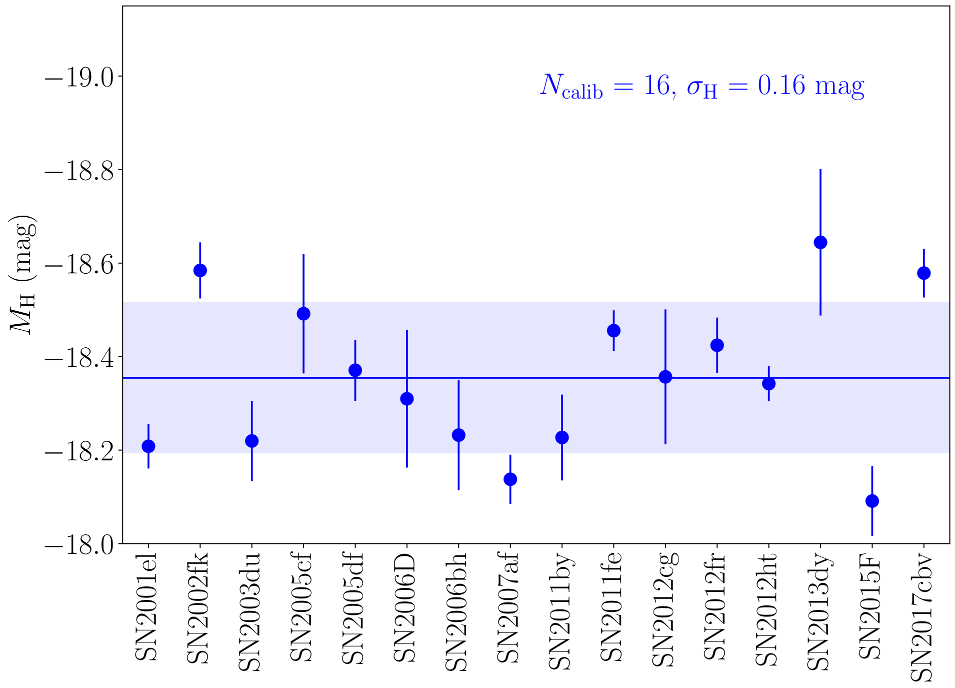

Apparent peak magnitudes and SHOES Cepheid distances

Similar scatter to Dhawan+18, also in the H-band

Hubble flow

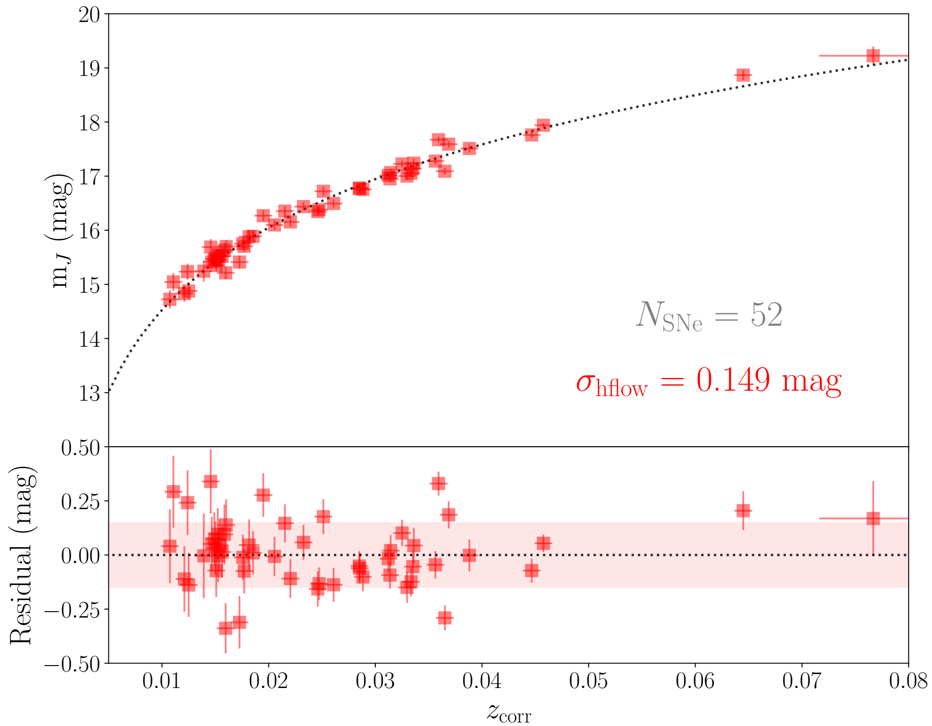

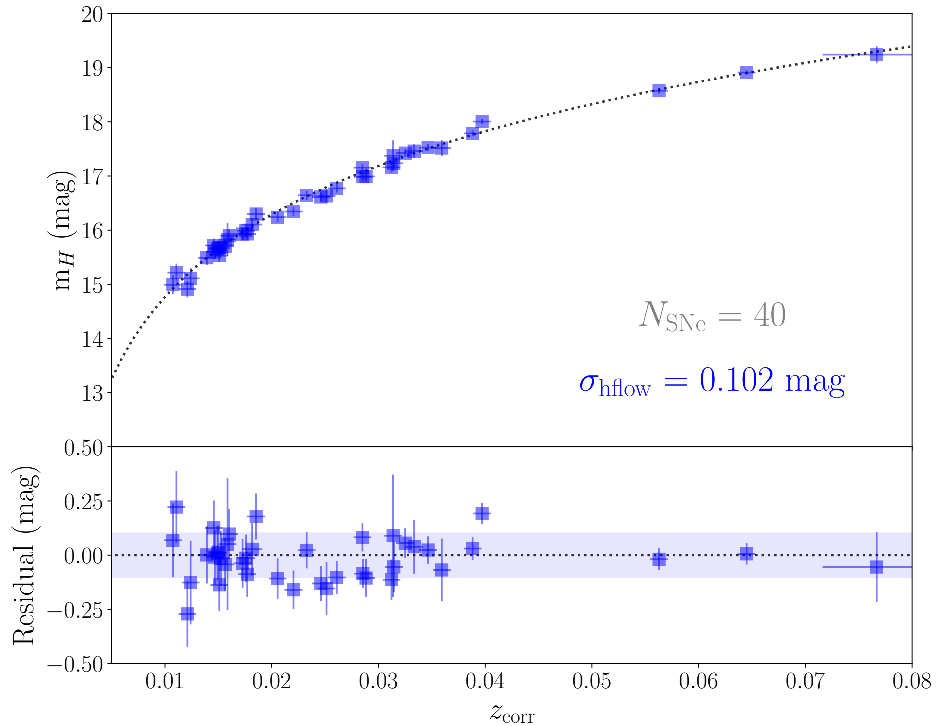

Apparent peak magnitude + LCDM (H0=70) cosmology w/ PV corr.

Lower scatter in H compared to J

H_0 detemination

Calibrator and Hubble flow samples combined to determine H_0, aX, and σ_{int}

$$\log_{10} H_0 = \frac{M_X + 5a_X + 25}{5}$$

With the likelihood

$$\log \mathcal{L} = -\frac{1}{2}\sum_i \frac{\log(2\pi\sigma^2_{\mathrm{Cal},i}) + (M_{\mathrm{Cal},i} - M_X)^2}{\sigma^2_{\mathrm{Cal},i}}$$

$$-\frac{1}{2}\sum_i \frac{\log(2\pi\sigma^2_{\mathrm{HF},i}) + (M_{\mathrm{HF},i} - M_X + 5\log(H_0/70))^2}{\sigma^2_{\mathrm{HF},i}}$$

$$\sigma^2_{\mathrm{Cal},i} = \sigma^2_{M_{X,i}} + \sigma^2_{int} \qquad \sigma^2_{\mathrm{HF},i} = \sigma^2_{M_{X,i}} + \sigma^2_{int}$$

$$H_0^J = 72.31^{+1.42}_{-1.42}\ \mathrm{km\ s^{-1}\ Mpc^{-1}}$$

$$\sigma^J_{int} = 0.125^{+0.017}_{-0.015}$$

$$H_0^H = 72.34^{+1.33}_{-1.25}\ \mathrm{km\ s^{-1}\ Mpc^{-1}}$$

$$\sigma^H_{int} = 0.096^{+0.016}_{-0.014}$$

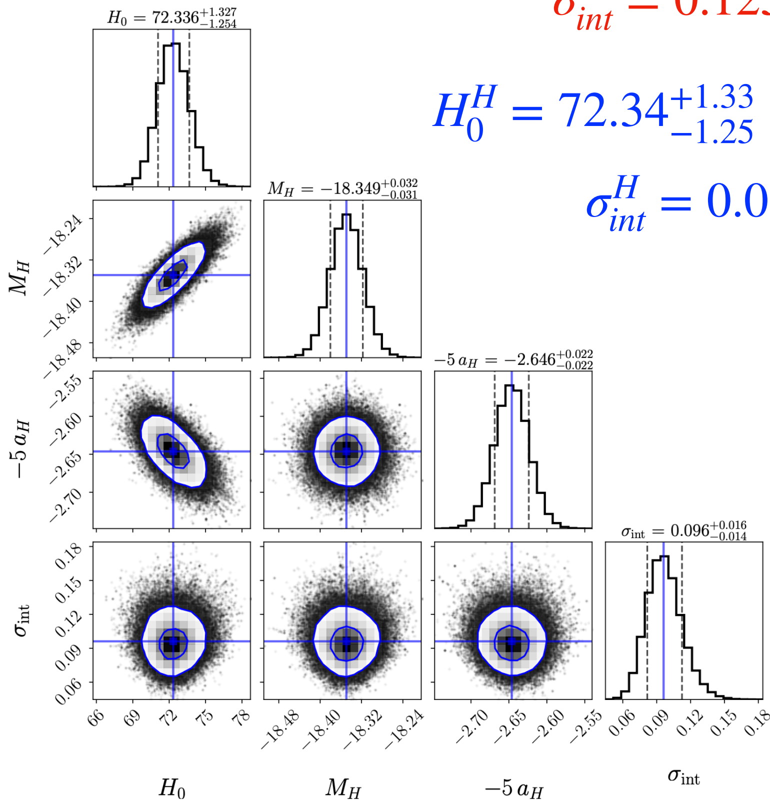

Systematics: 1.44 km/s/Mpc

(1) Dispersion of 21 variations from the baseline

Table 3. Results of MCMC posteriors for our baseline analysis and the 21 variations.

Variation	$N_{\rm cal}$	$\sigma_{\rm cal}$ (mag)	$N_{\rm HF}$	$\sigma_{\rm HF}$ (mag)	H_0 (km s^{-1} Mpc^{-1})	M_X (mag)	$-5a_X$ (mag)	$\sigma_{\rm int}$ (mag)	ΔH_0 (%)
					J-band				
Baseline	19	0.160	52	0.149	$72.31^{+1.42}_{-1.42}$	$-18.58^{+0.04}_{-0.04}$	$-2.87^{+0.02}_{-0.02}$	$0.125^{+0.017}_{-0.015}$	…
v_{pec} = 350 km s^{-1}	19	0.160	52	0.149	$72.36^{+1.41}_{-1.40}$	$-18.57^{+0.04}_{-0.03}$	$-2.87^{+0.02}_{-0.02}$	$0.117^{+0.018}_{-0.015}$	0.07
v_{pec} = 150 km s^{-1}	19	0.160	52	0.149	$72.26^{+1.51}_{-1.45}$	$-18.57^{+0.04}_{-0.04}$	$-2.87^{+0.02}_{-0.02}$	$0.135^{+0.015}_{-0.014}$	−0.07
v_{pec} = 0 km s^{-1}	19	0.160	52	0.149	$72.16^{+1.55}_{-1.50}$	$-18.58^{+0.04}_{-0.04}$	$-2.87^{+0.02}_{-0.02}$	$0.145^{+0.015}_{-0.013}$	−0.21
z_{cmb}	19	0.160	52	0.152	$71.53^{+1.45}_{-1.39}$	$-18.57^{+0.04}_{-0.04}$	$-2.85^{+0.02}_{-0.02}$	$0.124^{+0.017}_{-0.015}$	−1.08
z_{corr} from NED+C15	19	0.160	52	0.161	$71.96^{+1.42}_{-1.41}$	$-18.57^{+0.04}_{-0.04}$	$-2.86^{+0.02}_{-0.02}$	$0.125^{+0.018}_{-0.016}$	−0.48
z_{cmb} from NED	19	0.160	52	0.145	$71.62^{+1.36}_{-1.37}$	$-18.57^{+0.03}_{-0.04}$	$-2.85^{+0.02}_{-0.02}$	$0.116^{+0.016}_{-0.015}$	−0.95
z_{corr} from REF+C15	19	0.160	52	0.165	$72.05^{+1.49}_{-1.47}$	$-18.57^{+0.04}_{-0.04}$	$-2.86^{+0.02}_{-0.02}$	$0.132^{+0.018}_{-0.016}$	−0.36
z_{cmb} from REF	19	0.160	52	0.148	$71.60^{+1.39}_{-1.36}$	$-18.57^{+0.04}_{-0.04}$	$-2.85^{+0.02}_{-0.02}$	$0.121^{+0.017}_{-0.015}$	−0.99
$E(B-V) < 0.3$	18	0.162	44	0.141	$72.72^{+1.44}_{-1.42}$	$-18.58^{+0.04}_{-0.04}$	$-2.89^{+0.02}_{-0.02}$	$0.117^{+0.017}_{-0.015}$	0.56
HF $z > 0.023$	19	0.160	24	0.136	$72.99^{+1.64}_{-1.63}$	$-18.58^{+0.04}_{-0.04}$	$-2.89^{+0.03}_{-0.03}$	$0.132^{+0.021}_{-0.018}$	0.94
HF $0.023 < z < 0.05$	19	0.160	22	0.128	$73.47^{+1.65}_{-1.64}$	$-18.58^{+0.04}_{-0.04}$	$-2.91^{+0.03}_{-0.03}$	$0.131^{+0.021}_{-0.018}$	1.61
no Chauvenet	19	0.160	55	0.185	$71.37^{+1.64}_{-1.65}$	$-18.57^{+0.04}_{-0.04}$	$-2.84^{+0.02}_{-0.03}$	$0.157^{+0.019}_{-0.017}$	−1.31
only best fits	17	0.167	42	0.151	$71.82^{+1.57}_{-1.53}$	$-18.58^{+0.04}_{-0.04}$	$-2.86^{+0.03}_{-0.03}$	$0.133^{+0.019}_{-0.017}$	−0.68
all gp	19	0.170	50	0.152	$72.90^{+1.44}_{-1.45}$	$-18.57^{+0.04}_{-0.04}$	$-2.88^{+0.02}_{-0.02}$	$0.126^{+0.017}_{-0.015}$	0.82
m_X from template	19	0.170	49	0.144	$73.94^{+1.38}_{-1.38}$	$-18.55^{+0.03}_{-0.03}$	$-2.90^{+0.02}_{-0.02}$	$0.120^{+0.017}_{-0.015}$	2.25
removing subluminous	19	0.160	49	0.144	$73.20^{+1.37}_{-1.38}$	$-18.57^{+0.03}_{-0.03}$	$-2.90^{+0.02}_{-0.02}$	$0.116^{+0.017}_{-0.015}$	1.22
only CSP	8	0.176	29	0.130	$75.09^{+2.07}_{-2.07}$	$-18.48^{+0.05}_{-0.05}$	$-2.86^{+0.03}_{-0.03}$	$0.113^{+0.022}_{-0.019}$	3.85
only CfA	4	0.062	22	0.145	$73.53^{+2.41}_{-2.35}$	$-18.53^{+0.07}_{-0.07}$	$-2.86^{+0.02}_{-0.02}$	$0.060^{+0.030}_{-0.032}$	1.69
only CSP+CfA	11	0.154	40	0.127	$75.07^{+1.72}_{-1.72}$	$-18.48^{+0.04}_{-0.04}$	$-2.86^{+0.02}_{-0.02}$	$0.100^{+0.018}_{-0.016}$	3.82
only spirals in HF	19	0.160	39	0.135	$73.43^{+1.44}_{-1.40}$	$-18.57^{+0.03}_{-0.03}$	$-2.90^{+0.02}_{-0.02}$	$0.115^{+0.018}_{-0.016}$	1.54
SHOES selection	19	0.160	18	0.117	$74.02^{+1.70}_{-1.67}$	$-18.57^{+0.04}_{-0.04}$	$-2.92^{+0.03}_{-0.03}$	$0.123^{+0.022}_{-0.018}$	2.36

72.72 ± 1.08 km s^{-1} Mpc^{-1}

72.32 ± 1.08 km s^{-1} Mpc^{-1}

1.08 km/s/Mpc

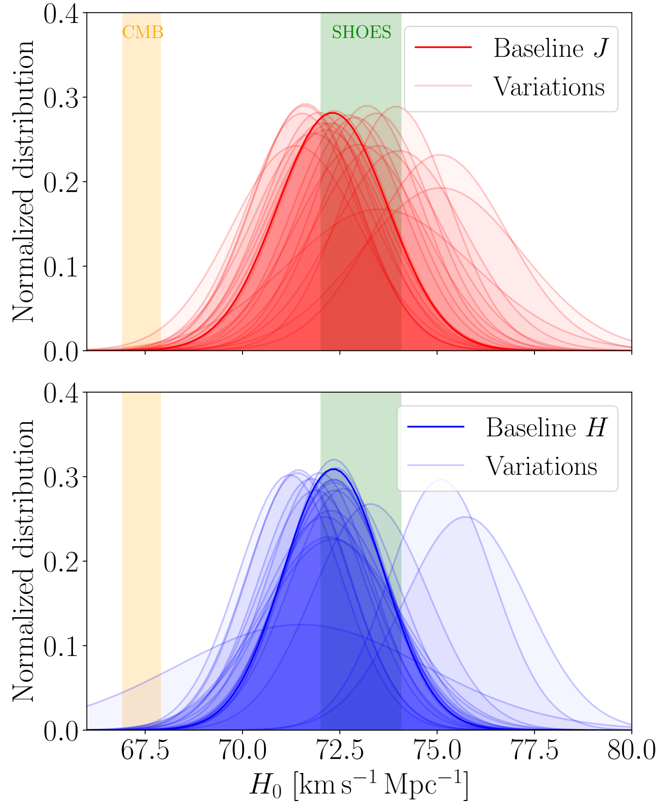

(2) Distance scale anchor systematic from R22: 0.7% of H0, 0.51 km/s/Mpc

(3) Photometric zero-point systematic: 0.02 mag, 0.7 km/s/Mpc

(4) PV uncertainties correlations on large scales: 0.5%, 0.4 km/s/Mpc

NIR Standardization?

Explored applying typical optical stretch and reddening corrections

$$M_i^{corr} = M_i - \alpha \times (\Delta m_{15,i} - 1) \qquad M_i^{corr} = M_i - \beta \times E(B-V)_i$$

Decreasing relation with stretch and reddening

Similar H_0 and clear improvement in σ_{int}

Variation	H_0 (km s^{-1} Mpc^{-1})	M_X (mag)	$-5a_X$ (mag)	$\sigma_{\rm int}$ (mag)	α	β
			J-band			
Baseline	$72.31^{+1.42}_{-1.42}$	$-18.58^{+0.04}_{-0.04}$	$-2.87^{+0.02}_{-0.02}$	$0.125^{+0.017}_{-0.015}$	...	...
Stretch corrected	$72.39^{+1.29}_{-1.27}$	$-18.61^{+0.03}_{-0.03}$	$-2.90^{+0.02}_{-0.02}$	$0.105^{+0.015}_{-0.014}$	$0.354^{+0.086}_{-0.086}$	...
Reddening corrected	$72.37^{+1.33}_{-1.31}$	$-18.61^{+0.04}_{-0.04}$	$-2.91^{+0.02}_{-0.02}$	$0.112^{+0.017}_{-0.015}$	...	$0.338^{+0.113}_{-0.115}$
Both corrections	$72.36^{+1.20}_{-1.19}$	$-18.64^{+0.03}_{-0.03}$	$-2.94^{+0.02}_{-0.02}$	$0.095^{+0.015}_{-0.013}$	$0.328^{+0.081}_{-0.081}$	$0.297^{+0.105}_{-0.106}$
			H-band			
Baseline	$72.34^{+1.33}_{-1.25}$	$-18.35^{+0.03}_{-0.03}$	$-2.65^{+0.02}_{-0.02}$	$0.096^{+0.016}_{-0.014}$	...	...
Stretch corrected	$72.22^{+1.26}_{-1.22}$	$-18.36^{+0.03}_{-0.03}$	$-2.66^{+0.02}_{-0.02}$	$0.094^{+0.017}_{-0.015}$	$0.133^{+0.094}_{-0.097}$	...
Reddening corrected	$72.44^{+1.31}_{-1.25}$	$-18.36^{+0.03}_{-0.03}$	$-2.66^{+0.03}_{-0.03}$	$0.094^{+0.017}_{-0.015}$	...	$0.108^{+0.116}_{-0.121}$
Both corrections	$72.32^{+1.30}_{-1.25}$	$-18.37^{+0.04}_{-0.03}$	$-2.67^{+0.03}_{-0.03}$	$0.092^{+0.017}_{-0.015}$	$0.137^{+0.095}_{-0.092}$	$0.115^{+0.118}_{-0.119}$

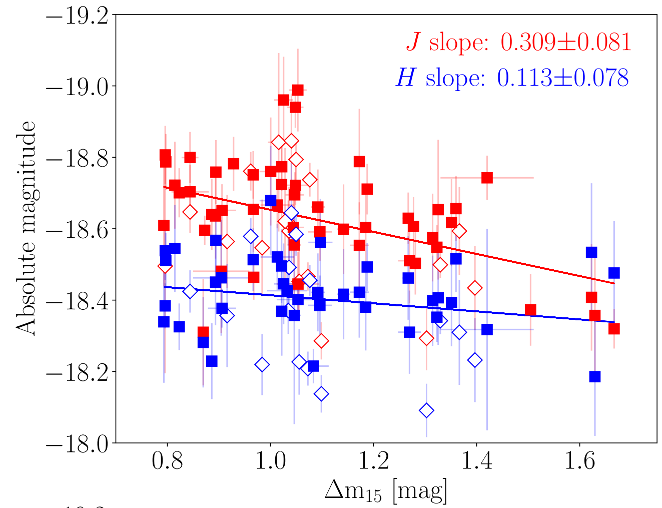

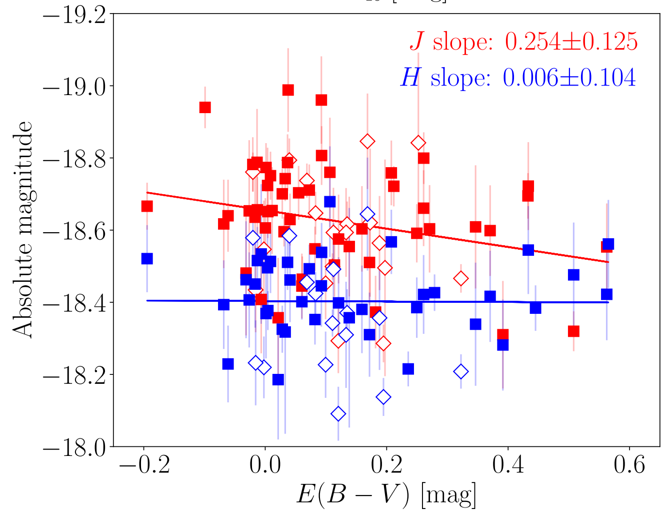

	Stretch	**Reddening**
B	**0.63±0.13**	**2.30±0.18**
r	**0.49±0.11**	**1.23±0.15**

Summary

LG, de Jaeger, Riess, …Leibundgut…et al.
2023A&A...679A..95G

- Our final result of H_0 is **72.31±2.02** km/s/Mpc in J (2.8% uncertainty), and **72.34±1.96** km/s/Mpc in H (2.7% uncertainty), both below the 3% precision

- This independent analysis confirms that SNe Ia in the optical do not introduce any bias in the H_0 measurement due to systematic uncertainties introduced in their standardization

- To improve the precision in H_0 we will need to:
  (i) increase number of calibrators (**JWST**)
  (ii) increase number of well-observed Hubble-flow SNIa (**Roman**)
  (iii) further study the NIR standardization of SNe Ia

Future work:

- Explore 3rd correction: **environment**
- The ***Aarhus-Barcelona*** FLOWS project
- SAINTS: a NIR SNIa Pantheon-like

Müller-Bravo & Galbany 2022

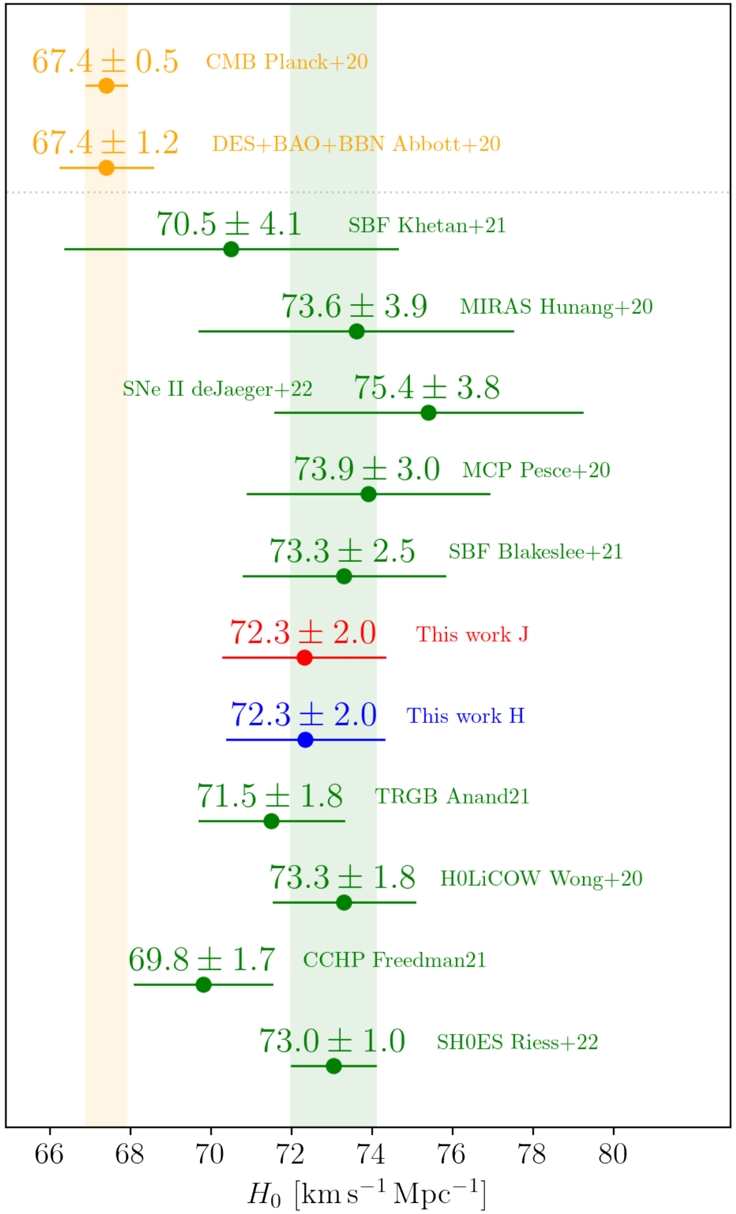

IFS of SN host galaxies

	PMAS	MUSE
Field of view	70”x70”	60”x60”
Spectral Resolution	R~500-1200	R~1700-3500
Number of spectra	~5,000 sp	~90,000 sp
Spatial Resolution	1”/spaxel	0.2”/spaxel
Wavelength coverage	3700-7500	4650-9300

More than 1000 SNIa host galaxies available (including SHOES)

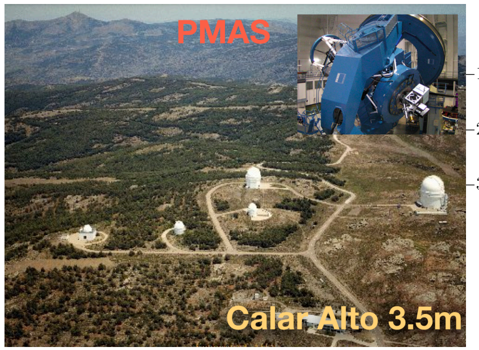

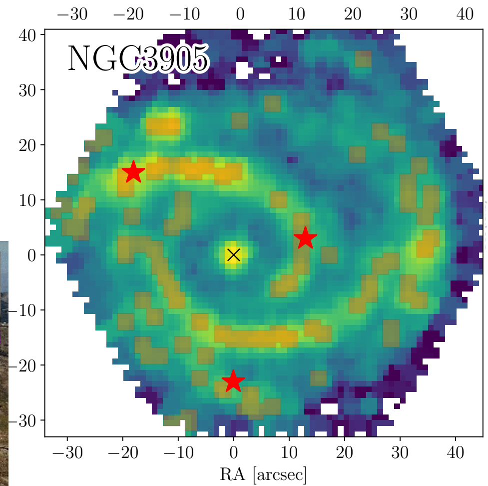

PISCO
Galbany+18

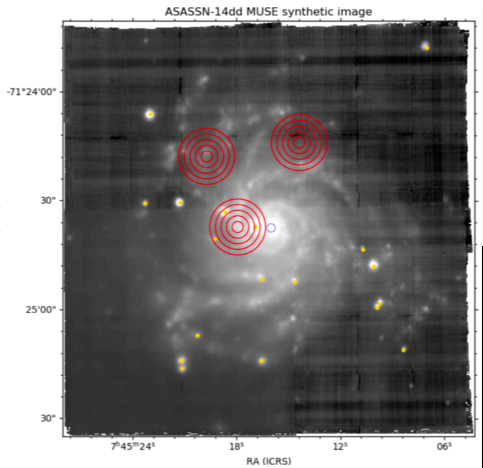

AMUSING
Galbany+16

The Aarhus-Barcelona FLOWS project

Transient Survey (ZTF)

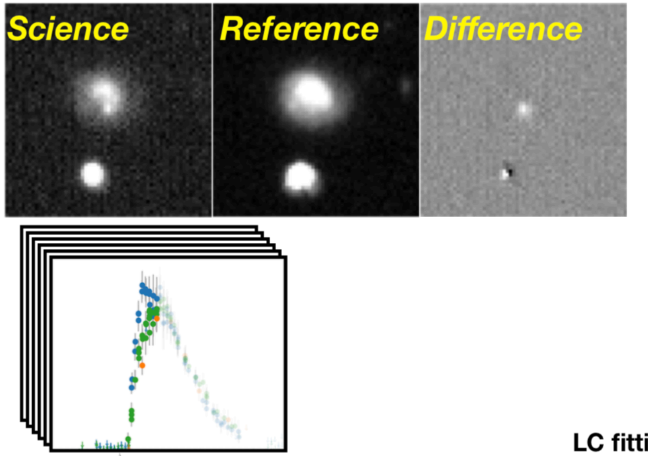

Broker

Trigger

LC fitting

HOSTFLOWS SNIa @ z=0.034

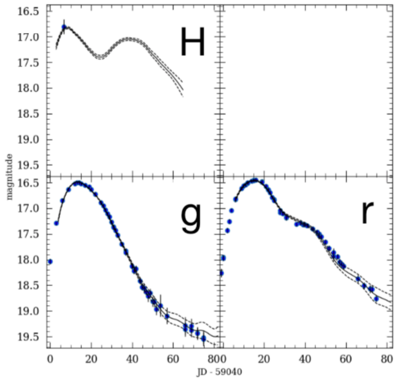

x ~200/year

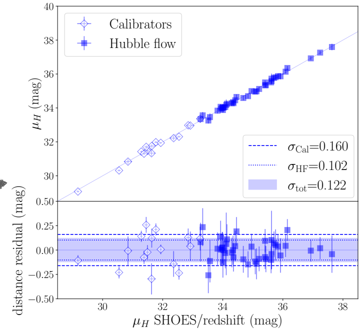

a. Build a new distance ladder in the NIR

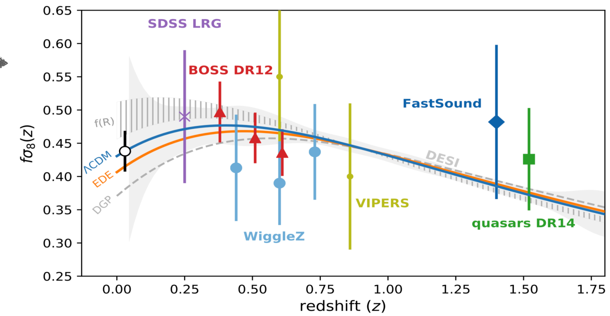

b. Independent estimate of σ_8 from pec. vel.

Simulation with CSP

Müller-Bravo, LG, et al. 2022A&A...665A.123M

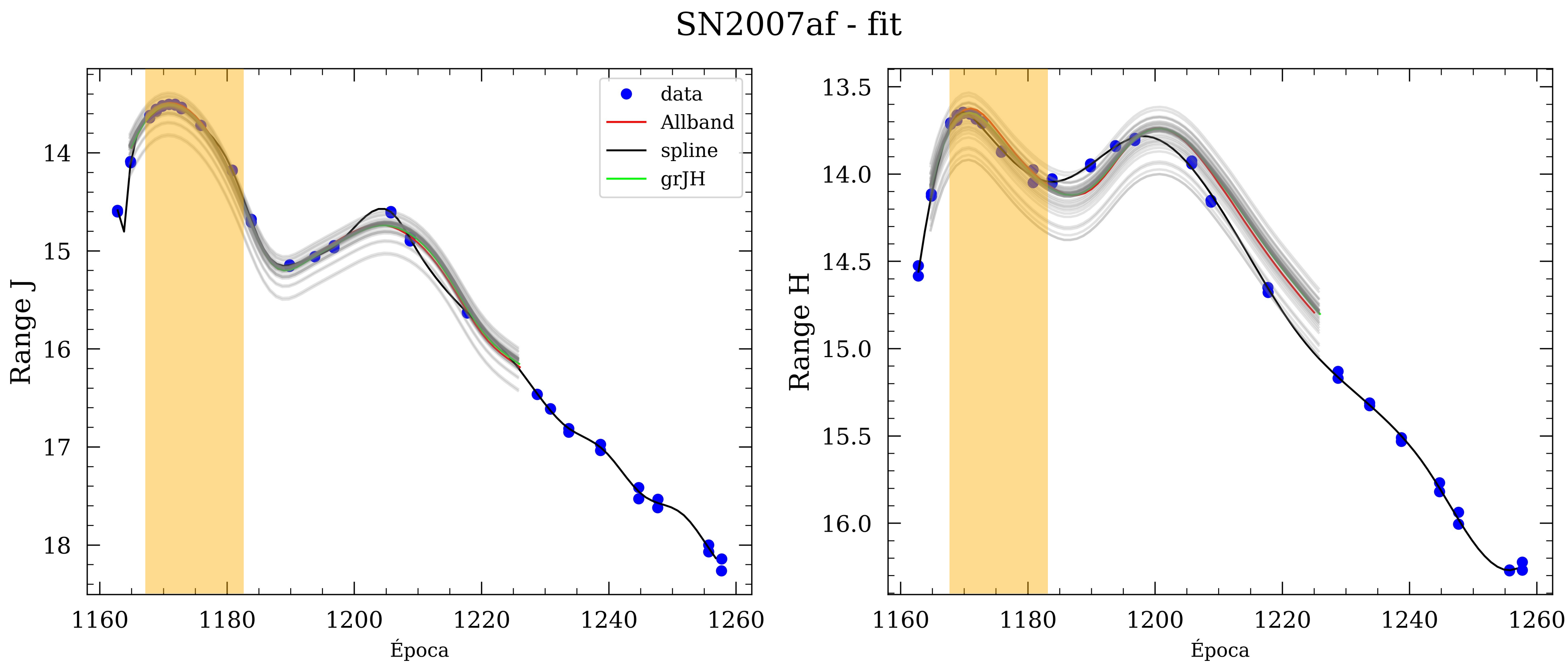

FLOWS Simulation with CSP

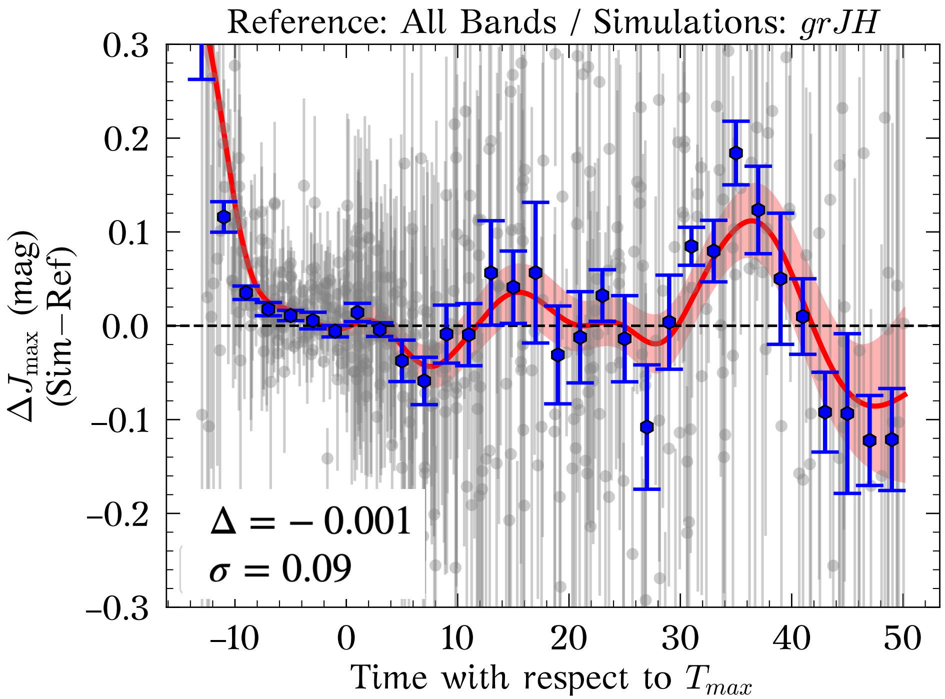

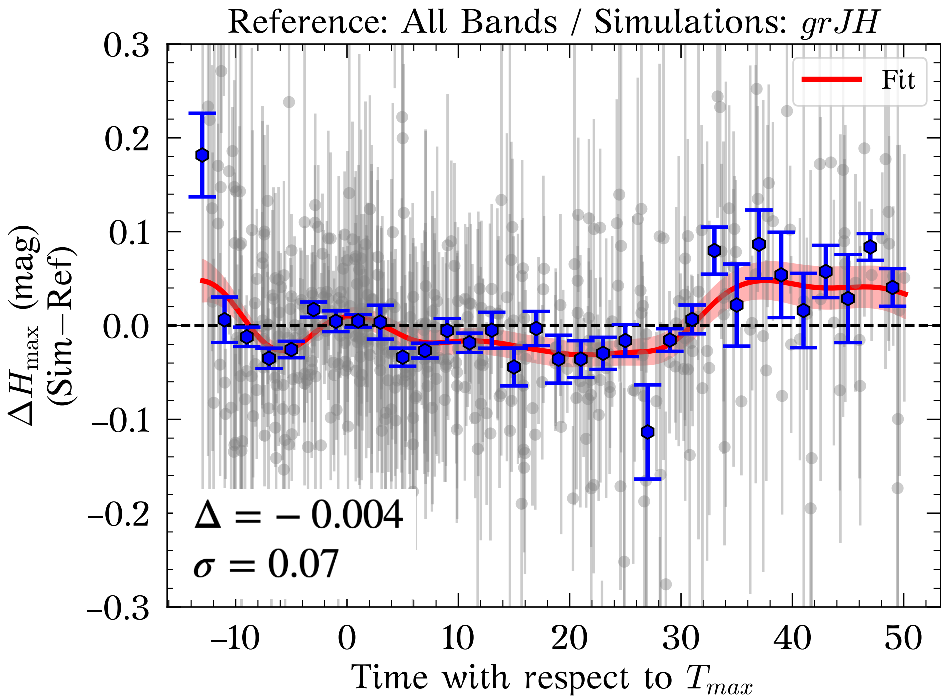

The Aarhus-Barcelona FLOWS project

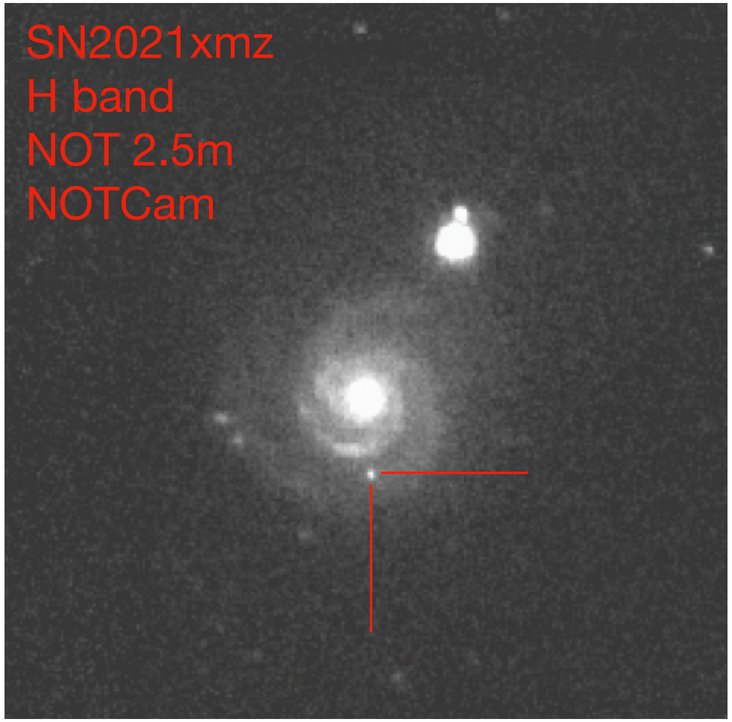

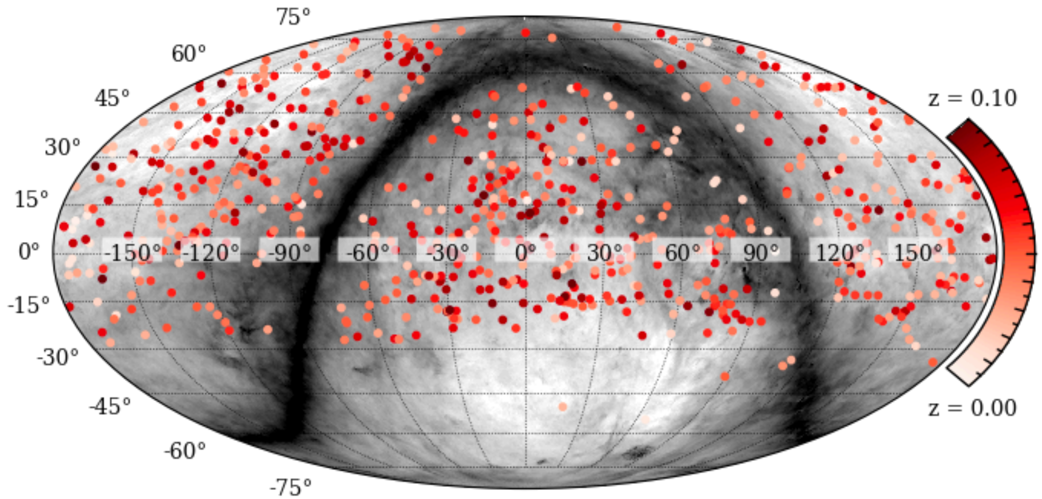

Optical light-curves:

gr from ZTF, *co* from ATLAS, *BVI* from TJO

\+ 1-3 JH epochs:

VLT-8.1m HAWKI
NTT-3.5m SOFI
CAHA-3.5m Omega2000
NOT-2.5m NOTCam
CMO-2.5m NIRCam
SPM-1.5m RATIR

757 SNe Ia already observed (*goal 1000)*

SAINTS


Erik Peterson


Joel Johansson


Tomás Müller


Matt Grayling


Suhail Dhawan


Aaron Do

Systematic Analysis Investigating NIR Type Ia Supernovae

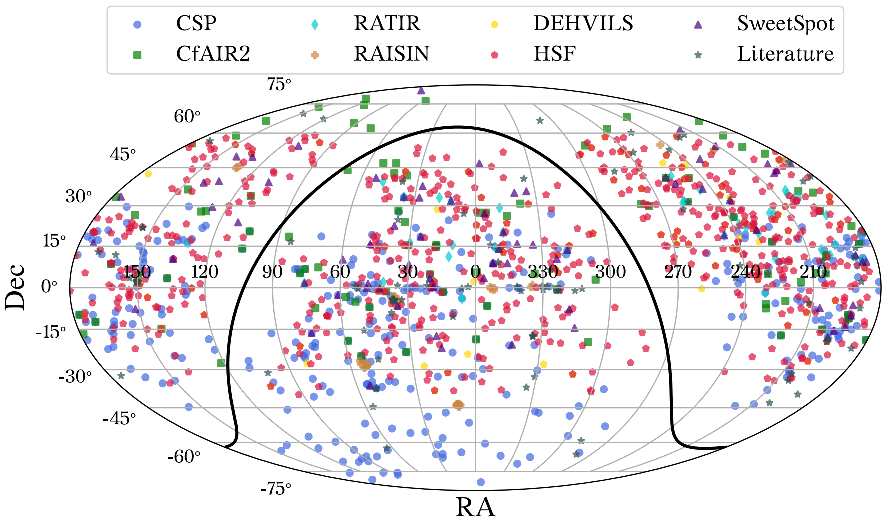

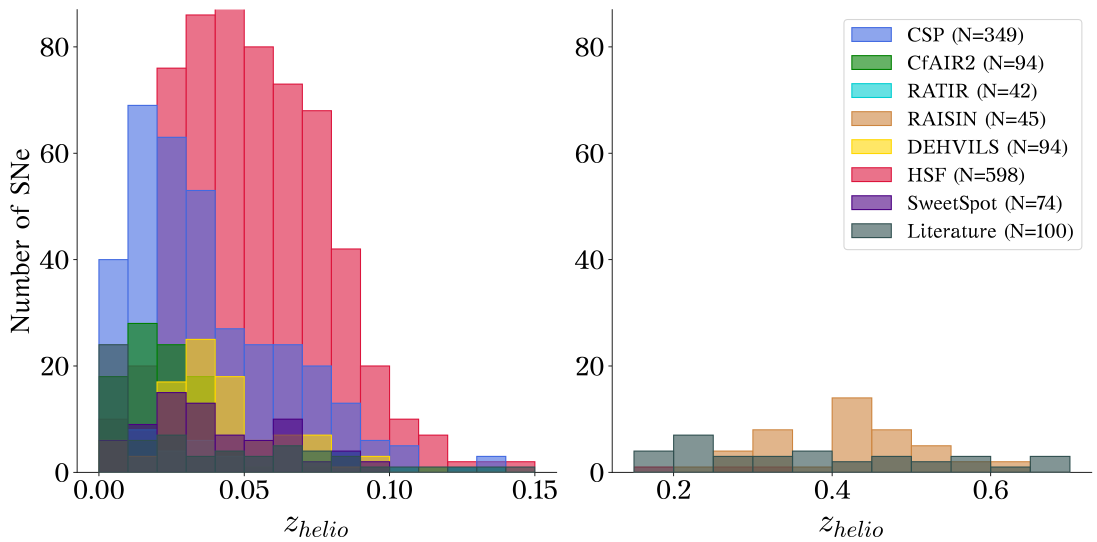

1222 SNe Ia in the NIR up to z~0.7

Full systematic analysis from published LC (recalibration, fitting, hosts…)

The Hubble constant from near-infrared observations of type Ia supernovae

Thanks!

Lluís Galbany, ICE-CSIC (Barcelona)

CosmoVerse, Napoli, 2025 May 23rd

Institute of Space Sciences

IEEC

CSIC
Consejo Superior de Investigaciones Científicas

Ministerio de Ciencia e Innovación

Unión Europea
Fondo Social Europeo
El FSE invierte en tu futuro

Agencia Estatal de Investigación